Asian Journal of Chemistry; Vol. 32, No. 11 (2020), 2783-2792

ASIAN JOURNAL OF CHEMISTRY

https://doi.org/10.14233/ajchem.2020.22827

New Copper(II) Complexes of Pyridine-2-carboxaldehyde-*N*-(2-pyridyl)hydrazone and 2-Hydroxy-1-naphthaldehyde-semicarbazone: Synthesis, Characterization, DNA Binding and Antimicrobial Activity Studies

OINAM U-WANG[1], RAJ KUMAR BHUBON SINGH[1,*], USAM IBOTOMBA SINGH[1], RAMINA[1], THOUDAM SURCHANDRA SINGH[1], TOKA SWU[2] and CH. BRAJAKISHORE SINGH[3]

[1]Department of Chemistry, Manipur University, Canchipur, Manipur-795003, India
[2]Department of Chemistry, Pondicherry University, Kalapet, Puducherry-605014, India
[3]Department of Biotechnology, Institute of Bioresources and Sustainable Development, Imphal-795001, India

*Corresponding author: E-mail: bhubonsingh@gmail.com

Received: 26 May 2020; *Accepted*: 17 July 2020; *Published online*: 28 October 2020; AJC-20102

Two new copper(II) complexes of pyridine-2-carboxaldehyde-*N*-(2-pyridyl)hydrazone $[Cu(PCPH)(H_2O)_2](NO_3)(H_2O)_2$ (**1**) and 2-hydroxy-1-naphthaldehyde-semicarbazone $[Cu(II)(HNSC)H_2O]\cdot NO_3\cdot H_2O$ (**2**) have been synthesized and characterized by spectroscopic techniques and single crystal X-ray diffraction study. Complex **1** crystallized as square pyramidal coordination complex in triclinic crystal system while complex **2** crystallized as square planar complex in monoclinic crystal system. EPR spectral patterns are of normal order of energy levels, *i.e.* $x^2\text{-}y^2 >> z^2 > xy > xz, yz$, with partial covalent character. Both copper(II) complexes were found to be groove binding to calf-thymus DNA and showed activity against *E. coli, S. aureus, B. cereus* and *E. faccium.*

Keywords: Copper(II), Hydrazone, Semicarbazone, DNA binding.

INTRODUCTION

sp^2 carbon rich flat aromatic rings are almost ubiquitous in medicinal chemistry [1]. It is due to the well characterized aromatic synthetic paths [2]. However, majority of aromatic moieties are heteroaromatic rings with polar surfaces [3] and amine and amide functionalities outside the ring structure have been added to enhance solubility [1], lower solubility and higher lipophilicity, leading to poorer efficacy and greater toxicity [2], remains a challenge for drugs containing aromatic moieties [4]. Also, the development of drug resistance and escape of microorganisms from the conventional antimicrobials call for new agents [5] and medicinal chemists have directed efforts toward metal-based drugs.

The formation of complexes increases the bioavailability of the metal ion or the ligand drug or both [6]. Many metal complexes of quinolone antibiotics, which inhibit bacterial DNA gyrase and topoisomerase IV required for DNA replication [7], *viz.* ciprofloxacin, norfloxacin and ofloxacin have been reported to possess enhanced activity rather than antibiotic alone [8,9]. Palladium(II) tetracycline complex has been reported sixteen times more potent than tetracycline against *E. coli* HB101/pBR322, a bacterial strain resistant to tetracycline and Pd(II) doxycycline complex is two times more potent than doxycycline against the same resistant strain [10].

Metal complexes of ligands containing aromatic moieties, can bind to DNA *via* intercalation and minor groove binding [11]. Among such ligands, aryl-/heteroaryl-/*N*-heteroaryl hydrazones have received significant attention due to their ligation property [12]. In continuation of our research on biologically active transition metal coordination complexes [13-20], we herein report the syntheses, spectroscopic characterization, crystal structures, DNA-binding study and antimicrobial activity of copper(II) complexes of pyridine-2-carboxaldehyde-*N*-(2-pyridyl)hydrazone $[Cu(PCPH)Cl(H_2O)](NO_3)(H_2O)_2$ (**1**) and 2-hydroxy-1-naphthaldehyde semicarbazone $[Cu(II)(HNSC)\text{-}H_2O]\cdot NO_3\cdot H_2O$ (**2**).

EXPERIMENTAL

All the chemicals were purchased from Sigma Aldrich and Himedia and used as received without further purification. Elemental (C, H, N) analysis were carried out using Perkin

Elmer 2400 II Elemental Analyzer. FTIR spectra (KBr pellets, 4000-400 cm^{-1}) were recorded on a Shimadzu FTIR 8400S spectrophotometer. UV-vis spectra as well as the absorption titration studies were recorded on Perkin Elmer Lambda 35 UV/VIS spectrophotometer. Perkin-Elmer LS 55 Fluorescence spectrophotometer was used in ethidium bromide-DNA fluorescence quenching experiment. Cyclic voltammetry measurements were carried out using a CH602C Electrochemical Analyzer against AgCl/Ag (saturated KCl) reference electrode. JEOL, JES-FA200 ESR spectrometer was used to record EPR spectra at RT and LNT. Sherwood scientific magnetic susceptibility balance calibrated with mercury(II)tetrathiocyanatocobaltate(III) was used to measure RT magnetic susceptibilities. Viscosity measurements in DNA-binding studies were carried out using Ostwald's viscometer immersed in a thermostated water bath at 298 K. The viscosities (η) of samples were determined using the equation:

$$\eta = (t - t_o)/t_o$$

where t_o is the flow time of buffer alone and t is the flow time of ct-DNA solutions with increasing concentrations of complex.

Synthesis of pyridine-2-carboxaldehyde-*N*-(2-pyridyl)-hydrazone (PCPH) and $[Cu(PCPH)(H_2O)_2](NO_3)(H_2O)_2$ (1): The PCPH ligand was prepared by refluxing pyridine-2-carboxaldehyde (1 mmol, 0.09 mL) and 2-hydrazinopyridine dihydrochloride (1 mmol, 0.18 g) in 20 mL methanol for 2 h. To the resulting yellow colour solution was added copper(II) nitrate trihydrate (1 mmol, 0.24 g) solution in 10 mL ethanol drop-wise and stirred overnight. On keeping the filtrate for slow evaporation, single crystals suitable for X-ray diffraction study were collected after 2 weeks. Colour: dark green. Yield: 0.30 g (70.58%). m.p.: (°C): 250-252. Anal. calcd. (found) % for $C_{11}H_{16}N_5O_9Cu$: C, 30.98 (30.95); H, 3.75 (3.70); N, 16.43 (16.40)%. UV-vis [H_2O, λ_{max}, nm (ε)]: 231 (100), 272 (100), 640 (2.7). FT-IR (KBr, ν_{max}, cm^{-1}): 3163 (-NH-), 1687 (C=N). Magnetic moment (27 ºC, μ_B): 1.72. Λ_M (water, 25 °C, S cm^2 mol^{-1}): 70.0.

Synthesis of 2-hydroxy-1-naphthaldehyde-semicarbazone (HNSC) and $[Cu(II)(HNSC)H_2O]\cdot NO_3\cdot H_2O$ (2): The HNSC ligand was synthesized by refluxing 2-hydroxy-1-naphthaldehyde (2 mmol, 0.34 g) and semicarbazide hydrochloride (2 mmol, 0.22 g) in 20 mL methanol for 2 h. To the resulting yellow colour solution was added copper(II) nitrate trihydrate (2 mmol, 0.482 g) solution in 20 mL ethanol dropwise and stirred for 2 h. On keeping the filtrate for slow evaporation single crystals of $[Cu(II)(HNSC)H_2O]\cdot NO_3\cdot H_2O$ (**2**) suitable for X-ray diffraction studies were collected after two weeks. Colour: dark green. Yield: 0.70 g (89.86%). m.p.: 218-221 ºC. Anal. calcd. (found) % for $C_{12}H_{14}N_4O_7Cu$: C, 36.90 (36.94); H, 3.55 (3.59); N, 14.34 (14.36). UV-vis [H_2O, λ_{max}, nm (ε)]: 291 (60), 363 (87), 585 (4.1). FT-IR (KBr, ν_{max}, cm^{-1}): 3333, 3193 ($-NH_2$), 3134 (-NH-), 1683 (C=O), 1663 (C=N). Magnetic moment (27 °C, μ_B): 1.73. Λ_M (water, 25 °C, S cm^2 mol^{-1}): 64.0.

Crystallographic data collection and refinement: X-ray crystallographic data were collected on Xcalibur, Eos diffractometer equipped with graphite monochromatized MoK_α radiation (λ = 0.7107 Å) at 298K. Data reduction and absorption correction were performed with CrysAlisPro, Version 1. 171.36.21 [21]. The structures were solved using SHELX-2008 [22] and refined with full-matrix-least-squares on F^2. Empirical absorption correction using spherical harmonics were implemented in SCALE3 ABSPACK scaling algorithm. Primary atoms were located by structure-invariant direct method. Hydrogen atom sites were inferred from neighboring sites. Molecular structure and crystallographic illustrations were prepared using OLEX-2-1.3 [23].

DNA-binding studies: For predicting the mode of ct-DNA binding of the newly synthesized complexes, electronic absorption titrations, fluorescence quenching experiment, cyclic voltammetric measurements and viscosity measurements were carried out.

Antimicrobial activity study: A Gram-negative and three Gram-positive bacteria and a species each of yeast and fungus were used for the antimicrobial assays. The strains were *Escherichia coli* (EC) ATCC-11229, *Staphylococcus aureus* (SA) ATCC-11632, *Bacillus cereus* (BC) MTCC-430, *Enterococcus faecium* (EF) ATCC-35667, *Candida albicans* (CA) ATCC-10231 and *Aspergillus niger* (AN) ATCC-16888. Microbial growth inhibitory potentials of the compounds were determined by Agar diffusion method and minimum inhibitory concentration (MIC) were determined by serial dilution method.

RESULTS AND DISCUSSION

The reported copper(II) complexes were synthesized by Schiff base condensation followed by reaction with copper(II) nitrate (Fig. 1). The complexes are soluble in water and other polar solvents. The molar conductance of copper(II) complexes **1** and **2** in water were found to be 70.0 and 64 S cm^2 mol^{-1}, respectively showing 1:1 electrolytic nature for both complexes.

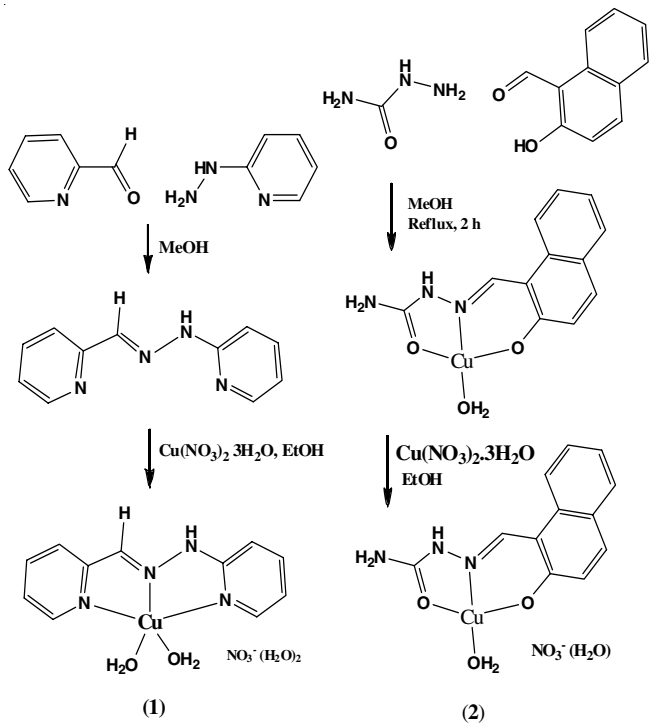

Fig. 1. Representative equations for syntheses of Cu(II) complexes **1** and **2**

FTIR, UV-vis and EPR spectroscopic studies

FTIR studies: The FTIR absorption bands of copper(II) complex **1** at 3136 cm^{-1} can be assigned to ν(-NH-) vibrations. The ν(C=N) bands are observed at 1687 cm^{-1}. Bands at 524 and 468 cm^{-1} are assigned tentatively to ν(Cu-N) vibrations [20].

The FTIR absorption bands of compound **2** at 3333 and 3193 cm^{-1} are assigned to ν(NH_2) vibrations. The band at 3134 cm^{-1} is assigned to –NH- stretching vibration. The ν(C=O) and ν(C=N) bands are observed at 1683 cm^{-1} and 1653 cm^{-1}. Bands at 565 cm^{-1} are assigned tentatively to Cu-N vibration and 450, 425 cm^{-1} to Cu-O vibrations [20].

UV-vis studies: UV-visible spectrum of Cu(II) complex **1** shows broad *d-d* bands at 640 nm (15625 cm^{-1}, ε = 2.7 M^{-1} cm^{-1}) characteristic of square base copper(II) complexes. The spectrum shows ligand to metal charge transfer transitions at 272 and 231 nm (ε = 100 M^{-1} cm^{-1}). UV-vis spectrum of Cu(II) complex **2** shows *d-d* band at 585 nm (17094 cm^{-1}, ε = 4.1 M^{-1} cm^{-1}) and LMCT transitions at 363 (ε = 87 M^{-1} cm^{-1}) and 291 nm (ε = 59 M^{-1} cm^{-1}) [20].

EPR studies: The EPR spectrum of complex **1** obtained in DMF at LNT (Fig. 2), is of characteristic mononuclear copper(II) complex. The trend $g_{\|} > g_{\perp} > 2.003$ indicates axial symmetry with unpaired electron in $d_{x^2-y^2}$ [24]. The $g_{\|}$ value was found to be less than 2.38 indicating significant covalent character in metal-ligand bonding. Bonding parameters (α^2, β^2, γ^2) and orbital reduction factors ($k_{\|}$ and $k_{\perp}$) were calculated from EPR parameters (Table-1). The in-plane σ covalency parameter α^2 value was found to be 0.42 suggesting that there is about 58% overlapping between ligand orbital and metal *d*-orbital [24]. The $k_{\|}$ is greater than $k_{\perp}$ ($k_{\|} > k_{\perp}$), showing the possibility of out-of-plane π bonding in the complex [25]. G value greater than 4 indicates normal order of energy levels, *i.e.* $x^2-y^2 >> z^2 > xy > xz, yz$ [26]. The EPR spectrum of complex **2** obtained in DMF at LNT (Fig. 3), also shows similar characteristics with 14% overlapping between ligand orbital and metal *d*-orbital and normal order of energy levels (Table-1).

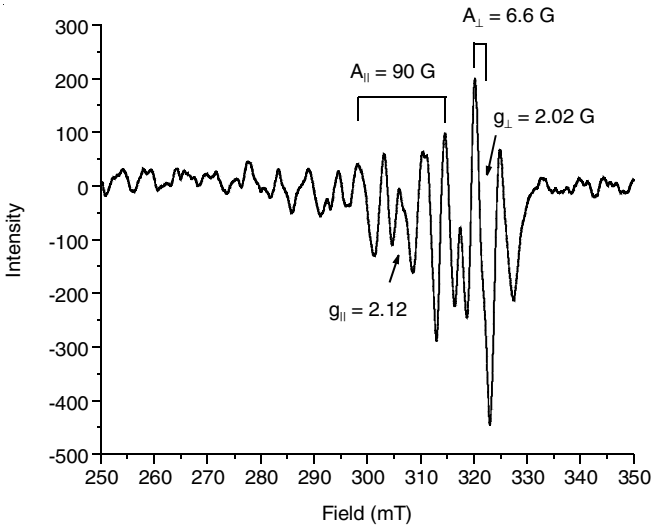

Fig. 2. EPR spectrum of Cu(II) complex **1** obtained from frozen DMF solution at LNT

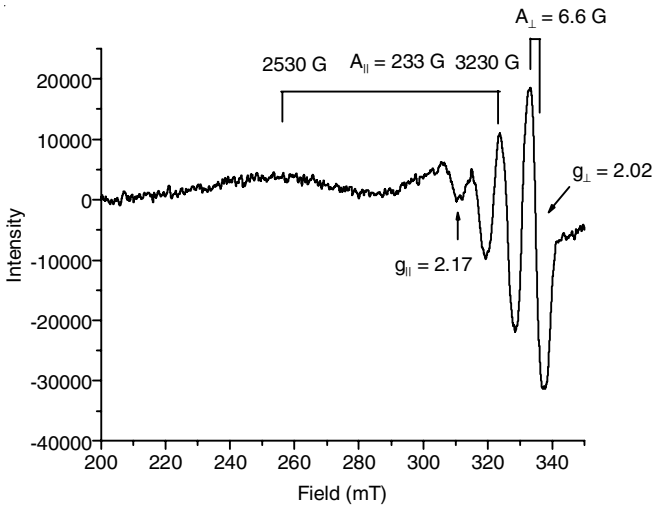

Fig. 3. EPR spectrum of Cu(II) complex **2** obtained from frozen DMF solution at LNT

X-ray diffraction studies of complexes 1 and 2: Crystal data and structure refinement are given in Table-2. The complex **1** crystallizes in space group *P*-1 of triclinic crystal system as $[Cu(PCPH)(H_2O)_2](NO_3)(H_2O)_2$ in which the copper(II) is in a distorted square pyramidal structure (Table-2, Fig. 4). In the complex, the ligand PCPH functions as a tridentate ligand bonded through N12(pyridine), N3(imine) and N14(pyridine) forming five membered chelate rings. Three nitrogen atoms of PCPH (N12N3N14) and a oxygen atom (O5) of water molecule occupy four coordination sites of the square plane while a water molecule, bonded through O6 atom, occupies the apical site. Selected bond lengths and bond angles of complex **1** are given in Table-3. The imine C1-N3 bond (1.37(10) Å) is shorter than C10-N2 single bond (1.57(11) Å) and pyridine C16-N12 bond (1.40(14) Å). The metal nitrogen bond lengths are nearly the same [Cu1-N3 (1.95(8) Å), Cu1-N12 (1.97(9) Å, Cu1-N14 (2.00(8) Å)]. The basal bond angle N12-Cu1-N14 = 163.5(3)º is larger than N3-Cu1-O5 = 158.8(3)º. The structural parameter τ, which is given by (larger basal angle-smaller basal angle)/60, is 0.08 showing distortion from perfect square pyramid geometry (τ = 0 for perfectly square pyramidal and τ = 1 for perfectly trigonal bipyramdal geometry) [27].

TABLE-1
EPR BONDING PARAMETERS OF COPPER(II) COMPLEXES **1** AND **2** IN DMF AT 77 K

Complex	E_{d-d} (nm)	$g_{\|}$	$g_{\perp}$	g_{av}	$A_{\|}$ (G)	$A_{\perp}$(G)	α^2	$k_{\|}$	$k_{\perp}$	β^2	γ^2	G
1	640	2.12	2.02	2.05	90	6.6	0.42	0.53	0.44	1.26	1.04	6
2	585	2.17	2.02	2.07	233	6.6	0.86	0.66	0.45	0.76	0.52	8.5

$\alpha^2 = -(A_{\|}/0.036) + (g_{\|} - 2.0023) + 3(g_{\perp} - 2.0023)/7 + 0.04$; $k_{\|}^2 = (g_{\|} - 2.0023)\, E_{d-d}/8\lambda_o$; $k_{\perp}^2 = (g_{\perp} - 2.0023)\, E_{d-d}/2\lambda_o$; $k_{\|} = \alpha^2\beta^2$ and $k_{\perp} = \alpha^2\gamma^2$; $G = (g_{\|}-2)/(g_{\perp}-2)$. Here λ_o is one electron spin orbit coupling constant and is equal to 828 cm^{-1}.

TABLE-2
CRYSTAL DATA AND DETAILS OF STRUCTURE REFINEMENT OF COPPER(II) COMPLEXES **1** AND **2**

	Complex **1**	Complex **2**
CCDC	1575942	918868
Empirical formula	$C_{11}H_{16}N_5O_9Cu$	$C_{12}H_{14}N_4O_7Cu$
Formula weight	425.83	389.81
T (K)	293	298
Crystal system	Triclinic	Monoclinic
Space group	*P*-1	$P2_1/n$
a (Å)	6.84(5)	11.80(7) Å
b (Å)	10.22(7)	6.67(4) Å
c (Å)	12.06(8)	19.05(14) Å
α (°)	88.61(6)	90.00
β (°)	82.40(6)	102.63(7)°
γ (°)	89.72(6)	90.00
V (Å^3)	835.14(10)	1484.1(3)
Z	2	4
ρ_{calc} (g cm^{-3})	1.693	1.745
μ (mm^{-1})	1.367	1.518
F_{000}	436.0	796.0
Crystal size/mm^3	0.34 × 0.034 × 0.04; block	0.19 × 0.11 × 0.06; block
Radiation	MoK$_\alpha$ (λ = 0.71073 Å)	MoK$_\alpha$ (λ = 0.71073 Å)
2θ range for data collection/°	7.58 to 50	6.4 to 50
Index Ranges	-8 ≤ h ≤ 8, -12 ≤ k ≤ 12, -13 ≤ l ≤ 14	-14≤ h ≤14, -8 ≤ k ≤ 8, -22≤ l ≤ 22
Reflections collected	7598	7186
Indipendent reflections	4536 [R_{int} = 0.0248, R_{sigma} = 0.0379]	2593 [R_{int} = 0.0496, R_{sigma} = 0.0637]
Data/restraints/parameters	4536/3/473	2593/0/228
Goodness-of-fit, S(F^2)	1.040	1.094
Final R indexes [I>=2σ (I)]	R_1 = 0.0344, wR_2 = 0.0894	R_1 = 0.0508, wR_2 = 0.1144
Final R indexes [all data]	R_1 = 0.0400, wR_2 = 0.0945	R_1 = 0.0796, wR_2 = 0.1282
Largest diff. peak/hole/e Å^{-3}	0.40/-0.39	0.72/-0.34

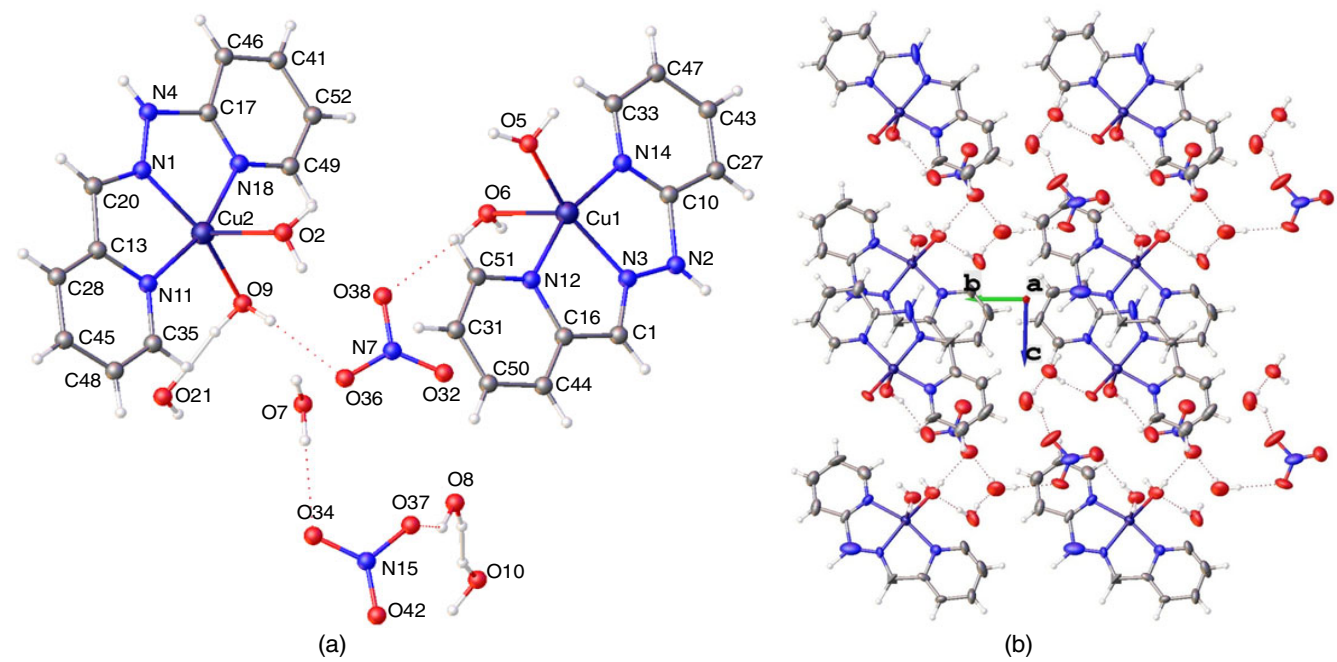

Fig. 4. (a) Crystallographic diagram of Cu(II) complex **1** with ellipsoids of 50% probability, (b) Packing diagram of Cu(II) complex **1** along a axis

The complex **2** crystallizes in space group $P2_1/n$ of monoclinic crystal system as [Cu(II)(HNSC)H_2O]·NO_3·H_2O in which the copper(II) is in a square planar structure (Table-2, Fig. 5). In the complex, the ligand HNSC functions as a tridentate ligand bonded through O1(amide), N1(imine) and O2(phenoxide) forming five membered and six chelate rings. The fourth coordination site is occupied by O2(water). The +2 charge of the copper atom is balanced by the phenoxide ion in the coordination sphere and a nitrate counter ion. Selected bond lengths and bond angles are given in Table-4. The C-O bond lengths

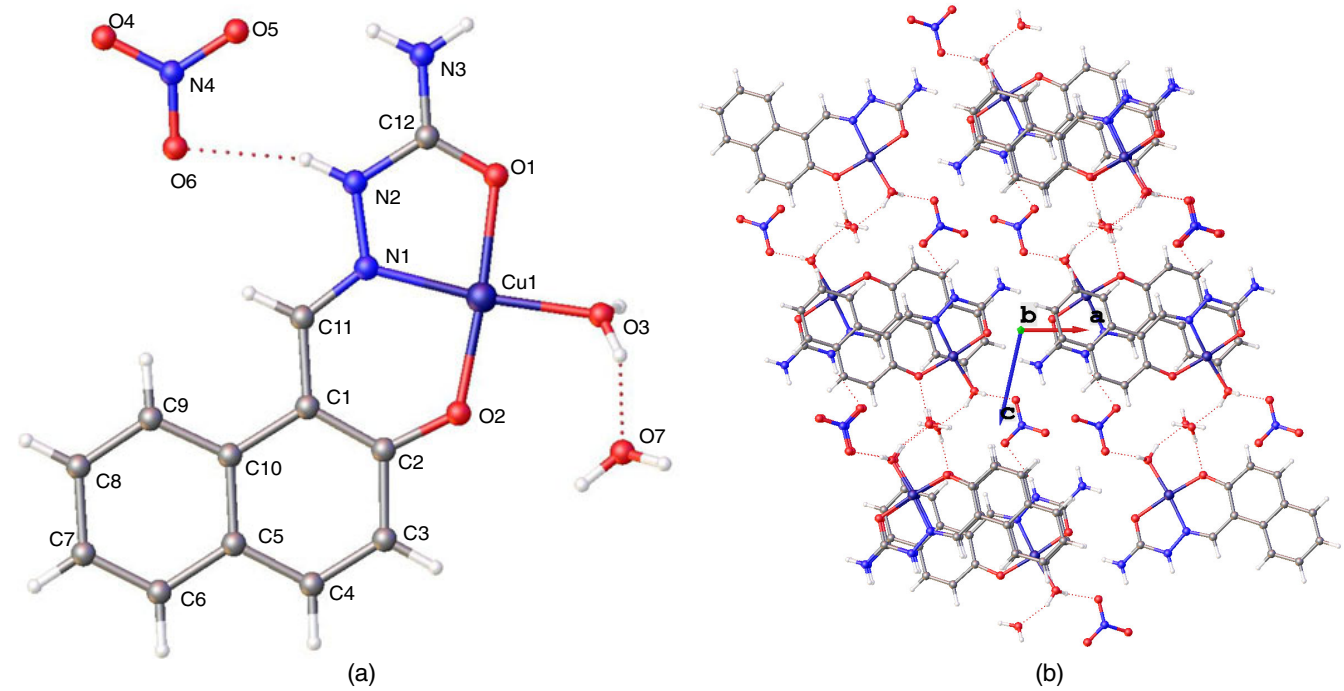

Fig. 5. (a) Crystallographic diagram of Cu(II) complex **2** with ellipsoids of 50% probability, (b) Packing diagram of Cu(II) complex **2** along b axis

TABLE-3
SELECTED BOND LENGTHS (Å) AND
BOND ANGLES (°) OF COPPER(II) COMPLEX **1**

Selected bonds	Bond length (Å)	Selected bond	Bond angle (°)
Cu1-N3	1.95 (8)	N3-Cu1-O6	108.2 (3)
Cu1-N12	1.97 (9)	N12-Cu1-O6	95.9 (3)
Cu1-N14	2.00 (8)	N14-Cu1-O6	90.6 (3)
Cu1-O5	1.96 (7)	N3-Cu1-N14	81.9 (3)
Cu1-O6	2.28 (8)	N3-Cu1-N12	82.0 (3)
C1-N3	1.37 (10)	N12-Cu1-N14	163.5 (3)
C10-N2	1.57 (11)	N3-Cu1-O5	158.8 (3)
N2-N3	1.33 (12)	N3-Cu1-O6	108.2 (3)
C16-C1	1.45 (13)	N12-Cu1-Cl5	95.3 (3)
C16-N12	1.40 (14)	O5-Cu1-O6	93.1 (3)
C16-C44	1.34 (15)	O5-Cu1-N14	99.1 (3)

TABLE-4
SELECTED BOND LENGTHS (Å) AND
BOND ANGLES (°) OF COPPER(II) COMPLEX **2**

Selected bonds	Bond length (Å)	Selected bond	Bond angle (°)
Cu1-O1	1.95 (3)	O2-Cu1-O1	175.45 (13)
Cu1-O2	1.88 (3)	O2-Cu1-O3	92.92 (17)
Cu1-O3	1.93 (4)	O2-Cu1-N1	93.01 (14)
Cu1-N1	1.90 (3)	O3-Cu1-O1	91.61 (18)
C12-O1	1.26 (5)	N1-Cu1-O1	82.42 (14)
C2-O2	1.33 (5)	N1-Cu1-O3	173.64 (17)
N1-N2	1.37 (5)	C12-O1-Cu1	112.4 (3)
N2-C12	1.36 (5)	C2-O2-Cu1	127.2 (3)
N3-C12	1.31 (6)	N2-N1-Cu1	112.2 (2)
N1-C11	1.30 (5)	C11-N1-Cu1	128.0 (3)
C11-C1	1.42(5)	C11-N1-N2	119.9 (4)
C1-C2	1.39 (6)	Cl2-N2-N1	114.4 (3)
C2-C3	1.42 (6)	O1-C12-N2	118.5 (4)
C3-C4	1.36 (6)	N3-C12-N2	118.5 (4)
C5-C10	1.41 (6)	O1-C12-N3	112.9 (4)
C5-C6	1.42 (6)	N1-C11-C1	124.4 (4)

in amide [C12-O1, 1.26 (5) Å] is shorter than that in phenoxide [C2-O2 1.33 (5) Å]. In semicarbazone N3-C12-N2-N1=C11 fragment, the bond lengths N3-C12 (1.31 (6) Å), C12-N2 (1.36 (5) Å), N2-N1 (1.37 (5) Å) and N1-C11 (1.30 (5) Å) are nearly the same. The metal-donor atom bond lengths are Cu1-O1 (1.95 (3) Å), Cu1-O2 (1.88 (3) Å), Cu1-O3 (1.93(4) Å) and Cu1-N1 (1.90 (3) Å). The bond angles around the metal center O2-Cu1-O1 (175.45 (13)°), N1-Cu1-O3 (173.64 (17)°), O2-Cu1-O3 (92.92 (17)°), N1-Cu1-O1 (82.42 (14)°) *etc*. show distortion in square planar geometry of the complex. The bond angles around C12 atom, N3-C12-N2 (118.5 (4)°), N2-C12-O1 (118.5 (4)°) and O1-C12-N3 (122.9°) (Table-4).

DNA-binding study

Electronic absorption titration: Electronic absorption titrations were carried out in Tris buffer solution (pH = 7.2). The absorbance ratio of ct-DNA solution in buffer at 260 and 280 nm was found to be 1.9, suggesting that the ct-DNA was satisfactorily free from protein [28]. The titrations were carried out by maintaining a constant concentration of the complex (5×10^{-4} M) and varying the concentration of ct-DNA solution added. The absorbance for each addition of ct-DNA was recorded subsequently. The intrinsic-binding constant, K_b, for complexes **1** and **2** were determined from eqn. 1:

$$\frac{[DNA]}{\varepsilon_a - \varepsilon_f} = \frac{[DNA]}{\varepsilon_b - \varepsilon_f} + \frac{1}{K_b(\varepsilon_b - \varepsilon_f)} \quad (1)$$

where, [DNA] is the concentration of DNA base pair which was calculated using molar absorption coefficient value 6600 $M^{-1}cm^{-1}$ for DNA at 260 nm [29], the apparent absorption coefficients ε_a, ε_f and ε_b corresponds to A_{obs}/[complex], extinction coefficients of complex in free and bound state, respectively. A plot of $[DNA]/(\varepsilon_a - \varepsilon_f)$ *vs.* [DNA] was used to calculate K_b from the ratio of slope and intercept [30].

Complex **1** (500 μM) in Tris buffer solution (pH = 7.2) shows charge transfer transitions at 272 nm Fig. 6a. The absorption spectra of complex **1** in the presence of ct-DNA (0-100 μM) displayed hypochromism at 272 nm and hyperchromism at 260 nm. The intrinsic-binding constant was calculated using absorbance values at 272 nm. The presence of isosbestic points in the spectra indicates the presence of more than one absorbing species in solution. Complex **2** (500 μM) in Tris-buffer solution (pH = 7.2) shows charge transfer bands at 347 and 265 nm Fig. 6b. The spectra in the presence of increasing concentration of ct-DNA (0-100 μM) displayed hypochromism at 347 nm and hyperchromism at 265 nm. The absorbance values at 347 nm were used to calculate intrinsic binding constant. The spectral patterns of complexes **1** and **2** were analogous to previously reported complexes whose interaction mode with DNA is non-intercalative and groove binding [16-18]. The intrinsic-binding constant, K_b for each complex was determined from the plot of $[DNA]/(\varepsilon_a - \varepsilon_f)$ *versus* [DNA] using eqn. 1. The slope to intercept ratio of the curves gave intrinsic-binding constant K_b of 2.4×10^4 M^{-1} for complex **1** and 8.7×10^4 M^{-1} for complex **2**. The K_b values are lower than those observed for classical intercalators (ethidium-DNA, 1.4×10^6 M^{-1} in 40 mM Na^+ ion concentration in 25 mM Tris-HCl (pH = 7.9) at 37 ºC [28-31]). The higher K_b value for complex **2** could be due to naphthalene moiety. The K_b values suggest weaker DNA-binding affinity of both Cu(II) complexes **1** and **2** than the classical intercalators [28-32]. The binding modes in both Cu(II) complexes were non-partially intercalative and groove or surface binding.

Fluorescence quenching experiment: Stock solution of protein free ($A_{260\,nm}/A_{280\,nm}$ = 1.9 [28]) ct-DNA in 5 mM Tris buffer (pH = 7.2) was freshly prepared and the concentration was calculated as 2×10^{-4} M using molar absorption coefficient value 6600 M^{-1} cm^{-1} of DNA at 260 nm [29]. Stock solutions of Cu(II) complexes **1** and **2** in water (2×10^{-4} M) and stock solution of ethidium bromide (EB) in water (3.3 μM) were prepared. Appropriate dilutions of the stock solutions were made for each experiment. In a typical experiment, 1.5 mL each of ethidium bromide solution was transferred into a series of vials. 25 μL each of ct-DNA (A_{260nm} = 2) were added to the ethidium bromide solutions. To the DNA-EB solutions in different vials, different volumes of complex (0, 10, 20, 30, *etc*., μM) were added. A total volume of 2.5 mL in each solution was maintained by adding additional volume of buffer. The solutions were equilibrated for 15 min. The variation in the fluorescence intensities with increasing concentration of complex were recorded at 605 nm over a spectra range of 500 to 750 nm using an excitation wavelength of 546 nm. The apparent binding constant K_{app} was calculated from eqn. 2:

$$K_{EB}[EB] = K_{app}[Complex] \quad (2)$$

where, $K_{EB} = 1.0 \times 10^7$ M^{-1}, [EB] = 2 μM and [Complex] = the molar concentration of complex at 50% reduction of fluorescence [33]. The classical Stern-Volmer quenching constants (K_{SV}) were calculated for each complex using the plot of linear Stern-Volmer equation:

$$\frac{I_o}{I} = 1 + K_{sv}r \quad (3)$$

where, I_o and I are the fluorescence intensities of DNA-EB in the absence and presence of the Cu(II) complex, respectively and r is the concentration ratio of Cu(II) complex to DNA [34,35]. K_{sv} value was obtained from the slope of a linear plot of I_o/I *vs*. r [35].

Ethidium bromide (EB) is a DNA intercalator [36] which gives significant fluorescence emission when intercalated between the adjacent DNA base pairs [32,35]. The extent of fluorescence quenching for ethidium bromide bound to DNA was used to study the extent of binding between the molecule and DNA [33,35,37]. Fig. 7a-b show the reductions in the fluorescence emission intensities of EB-DNA (2 μM) with increasing concentration of Cu(II) complexes **1** and **2** (0-100 μM) recorded in Tris buffer solution (pH = 7.2). Using eqn. 2

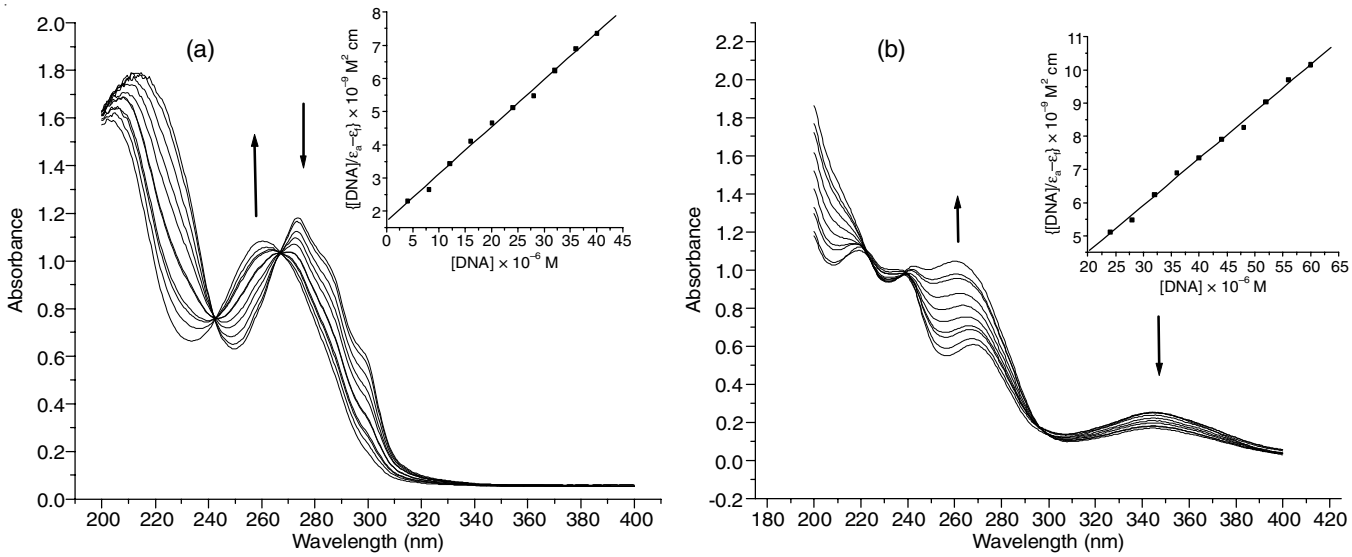

Fig. 6. (a) Electronic absorption titration of complex **1** (5×10^{-4} M) with ct-DNA (0-100 μM) in Tris-buffer (pH = 7.2); Inset: plot of $[DNA]/(\varepsilon_a - \varepsilon_f)$ *versus* [DNA]. (b) Electronic absorption titration of complex **2** (5×10^{-4} M) with ct-DNA (0-100 μM) in Tris-buffer (pH = 7.2); Inset: plot of $[DNA]/(\varepsilon_a - \varepsilon_f)$ *versus* [DNA]

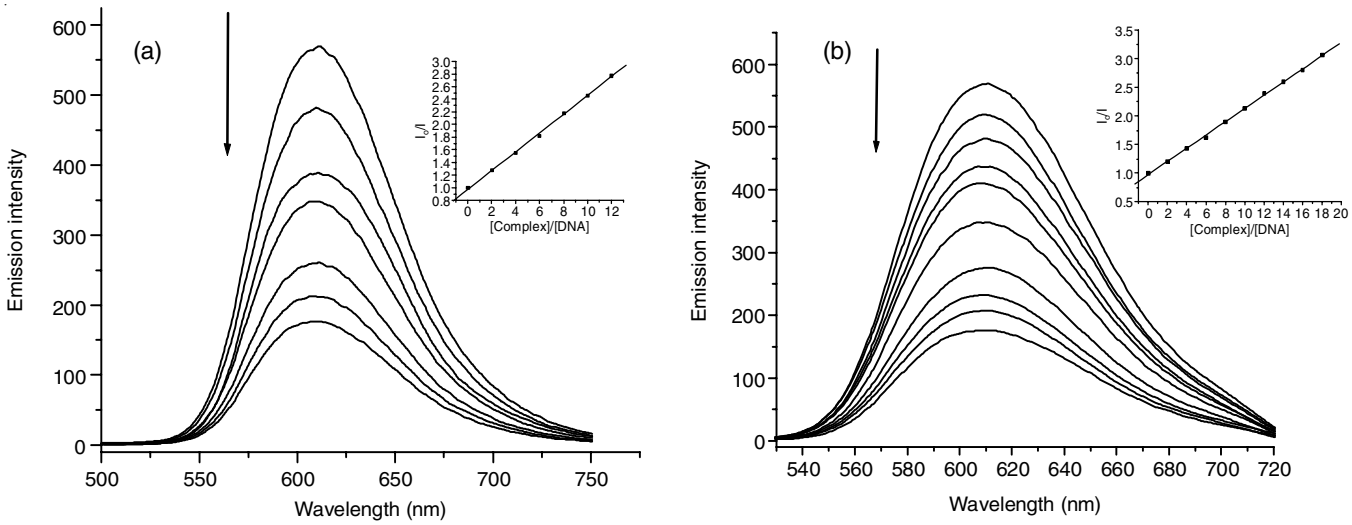

Fig. 7. (a) Fluorescence emission spectra of ethidium bromide-ctDNA in Tris-HCl buffer (pH = 7.2) with increasing concentration of Cu(II) complex **1** (λ_{ex} = 546 nm); Inset: Fluorescence quenching curve of EB-DNA by Cu(II) complex **1**. (b) Fluorescence emission spectra of ethidium bromide-ct-DNA in Tris-HCl buffer (pH = 7.2) with increasing concentration of Cu(II) complex **2** (λ_{ex} = 546 nm); Inset: Fluorescence quenching curve of EB-DNA by Cu(II) complex **2**

the apparent-binding constant K_{app} were calculated and found to be 3.5×10^5 M^{-1} and 3.7×10^5 M^{-1} for both Cu(II) complexes **1** and **2**, respectively. The observed values of K_{app} suggested the complexes were binding toward ct-DNA [33]. The quenching of EB-DNA fluorescence by the complexes is in good agreement with the linear Stern-Volmer equation (eqn. 3) [32]. The slope of the linear plot I_o/I *vs.* r (r = [Complex]/[DNA]) gave quen-ching constant K_{SV} values of 2.35 and 2.57 for Cu(II) comp-lexes **1** and **2**, respectively. The values suggest competitive inhibition caused by minor groove binding of the complexes, releasing some free ethidium bromide from DNA-EB complex and blocking potential interaction sites of ethidium bromide [32,35,38].

Cyclic voltammetry: Room temperature cyclic voltammogram of Cu(II) complex **1** (200 µM) *vs.* AgCl/Ag (saturated KCl) within +1.4 V to –1.4 V at a scan rate of 0.05 V/s in Tris buffer (pH = 7.2) in the absence of DNA gave two reduction peaks at 0.18 and –1.12 V, (Fig. 8a) which may be assigned to Cu(II)/Cu(I) and Cu(I)/Cu(0) reductions. The oxidation peaks in the reverse scan, observed at 0.18 and 0.75 V, were assigned to Cu(0)/Cu(I) and Cu(I)/Cu(II) oxidations, respectively. In the presence of ct-DNA (200 µM), a reduction peaks at –1.24 V and an oxidation peak at 1.12 V were observed. The peaks were tentatively assigned Cu(II)/Cu(I) couples. The formal potential $E_{1/2}$ values for Cu(II)/Cu(I) couple were observed as 0.18 V and -0.01 V in the absence and presence of DNA, respectively (Table-5).

From the wavy cyclic voltammogram of Cu(II) complex **2** (200 µM; Tris buffer pH = 7.2; +1.4 to –1.4V; 0.02 V/s) *vs.* AgCl/Ag (saturated KCl) in the absence of DNA two reduction

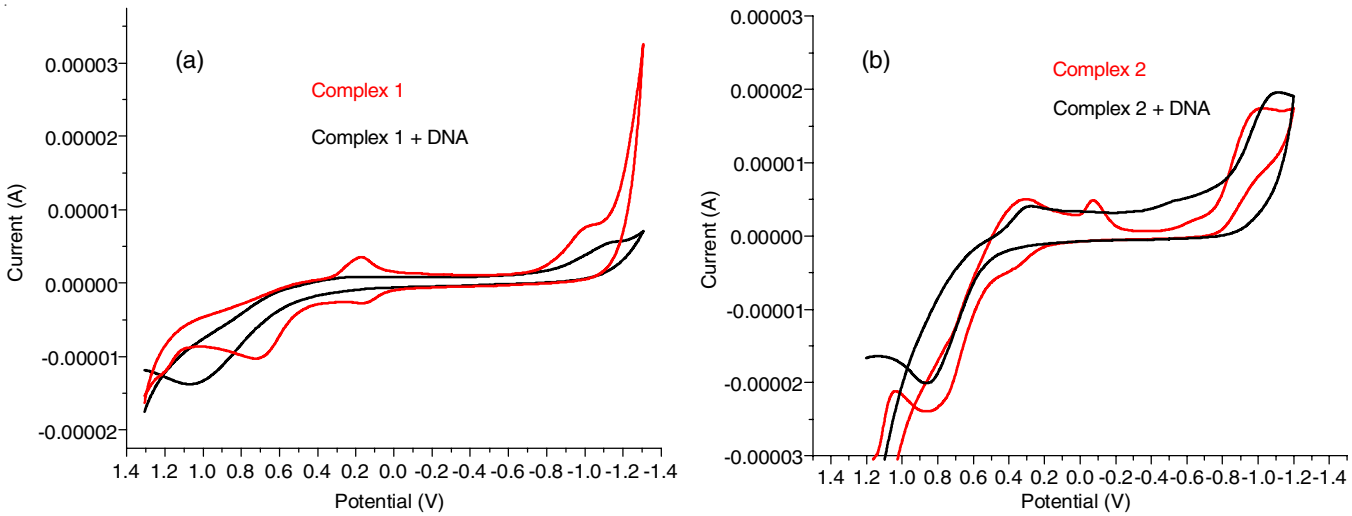

Fig. 8. (a) Cyclic voltammogram of Cu(II) complex **1** (200 µM) against AgCl/Ag (saturated KCl) electrode within +1.4 V to –1.4 V at a scan rate of 0.05 V/s in the absence (red) and presence (black) of ct-DNA (2×10^{-4} M). (b) Cyclic voltammogram of Cu(II) complex **2** (200 µM) against AgCl/Ag (saturated KCl) electrode within +1.4 V to –1.4 V at a scan rate of 0.02 V/s in the absence (red) and presence (black) of ct-DNA (2×10^{-4} M)

TABLE-5
CYCLIC VOLTAMMETRY DATA FOR COMPLEXES **1** AND **2** IN THE ABSENCE AND PRESENCE OF ct-DNA[a]

Complex	E_{PC} (V)	$i_{PC} \times 10^6$ (A)	E_{PA} (V)	$i_{PA} \times 10^6$ (A)	ΔE (V)	i_{PA}/i_{PC}	$E_{1/2}$ (V)
1	+0.18	3.39	+0.18	-2.75	0.0	0.81	0.18
	-1.12	7.91	+0.75	-10.30	1.87	1.30	-0.18
1 + DNA	-1.24	5.56	+1.12	-13.70	2.36	2.46	-0.01
2	+0.29	4.72	+0.37	-4.65	0.08	0.98	0.33
	-1.05	17.31	+0.86	-24.35	1.91	1.40	-0.11
2 + DNA	+0.28	4.16	+0.28	-1.52	0.0	0.36	0.28
	-1.12	19.39	+0.86	-20.13	1.98	1.03	-0.13

[a]E_{PA}, i_{PA} and E_{PC}, i_{PC} are anodic and cathodic peak potentials and peak currents; $\Delta E = E_{PA} - E_{PC}$ and $E_{1/2} = (E_{PA} + E_{PC})/2$.

peaks at 0.29 and –1.05 V (Fig. 8b) were assigned to Cu(II)/Cu(I) and Cu(I)/Cu(0) reduction processes. The corresponding oxidation peaks in the reverse scan were observed at 0.37 and 0.86 V. In the presence of DNA the Cu(II) complex **2** showed reduction peaks at 0.28 V (Cu(II)/Cu(I)) and -1.12 V (Cu(I)/Cu(0)). In the reverse scan oxidation peaks were observed at 0.28 V (Cu(0)/Cu(I)) and 0.86 V (Cu(I)/Cu(II)). The formal potential $E_{1/2}$ values for Cu(II)/Cu(I) couple were observed as 0.33 V and 0.28 V in the absence and presence of DNA, respectively (Table-5). The $E_{1/2}$ values for Cu(I)/Cu(0) in the absence and presence of DNA were -0.11 V and -0.13 V, respectively (Table-5).

For both Cu(II) complexes, the peak separation values and peak current ratios show that the redox processes are not reversible. As the DNA and the respective ligands do not show any redox processes it may be concluded that the redox processes are due to the presence of metal centers. The observed experimental result suggests that the presence of DNA strongly affects the redox processes of metal centers in both complexes. Among the three kinds of binding modes of small molecules to DNA, if the formal potential $E_{1/2}$ is shifted to more positive value the interaction mode is intercalative binding, while $E_{1/2}$ shifted to more negative value the binding mode is electrostatic [35]. It has been observed that the shift in $E_{1/2}$ values in presence of DNA from that in the absence of DNA are toward more negative values, suggesting the complexes bind to ct-DNA by non-intercalative surface or groove-binding mode through electrostatic interaction.

Viscosity measurement: Viscosity measurement of DNA solution with increasing concentrations of Cu(II) complex is useful for determining the binding mode of interaction of Cu(II) complex with DNA. The effects of small molecules on viscosity of DNA solution are as follows: Intercalative binding causes an increase in viscosity; non-classical intercalative binding causes a lowering in viscosity and surface or groove binding causes no change in viscosity of ct-DNA solution [16]. When viscosities of DNA solutions with increasing concentrations of complexes **1** and **2** were measured the relative viscosities (η/η_o) were found to be unchanged suggesting that complexes **1** and **2** binds with DNA *via* non-intercalative surface or groove binding.

Antimicrobial activity study

Tested microorganism: For the antimicrobial assays a Gram-negative and three Gram-positive bacterial and a species each of yeast and fungus were used. The strains of microorganisms tested were *Escherichia coli* (EC) ATCC-11229, *Staphylococcus aureus* (SA) ATCC-11632, *Bacillus cereus* (BC) MTCC-430, *Enterococcus faecium* (EF) ATCC-35667, *Candida albicans* (CA) ATCC-10231 and *Aspergillus niger* (AN) ATCC-16888.

Preparation of inoculum: Bacterial inoculums were prepared by growing cells in Luria Bertani Broth (HiMedia) for 24 h at 37 ºC. On the other hand, the inoculums of yeast and fugus strains were transferred directly into potato dextrose agar (HiMedia) plates and incubated at 25 ºC for 48 h. They were maintained on agar slant at 4 ºC and sub cultured on a fresh appropriate agar plates 24 h prior to any antimicrobial test. The Muller Hinton Broth (MHB) was used for the minimum inhibition concentration (MIC).

Determination of microbial growth inhibitory potential: The microbial growth inhibitory potentials of both Cu(II) complexes were determined by using the agar diffusion method [39] with some modification. Sterile Petri plates (90 mm) were prepared with 20-25 mL of sterile Luria Bertani Agar (LBA) (Himedia) and potato dextrose agar (PDA) (Himedia) and allowed to solidify. 100 µL of adjusted test cultures (10^8 CFU/mL) was swabbed on the top of the solidified media and allowed to dry for 10 min on the plates. Solidified plates were punched to make well of 6 mm diameter with the help of sterile coke borer. Next, 30 and 20 µL of each compound dissolved in dimethyl sulfoxide (DMSO; 5 mg/mL) were added into the wells. Gentamycin (5 µg/well) and nystatin (10 µg/well) (RA) 1 mg/mL in sterile distilled water were used as positive control for the bacteria and yeast, respectively. A well containing only DMSO (30 µL) was used as a negative control. Culture plates were incubated at 37 ºC for 24 h for bacteria and at 25 ºC for 48 h for yeast. At the end of the incubation, the diameters of the inhibition zone formed around the wells were measured in millimeter. The zone inhibition was increased with the increase in concentration of the compound and thus exhibiting concentration dependent activity. All tests were performed in triplicate (Table-6).

Determination of minimum inhibitory concentration (MIC): The MIC of Cu(II) complexes and reference antibiotic (RA) were determined as follows; the test sample was dissolved in 10% (v/v) DMSO/MHB to give a final concentration 500 µg/mL. This was serially diluted two-fold to obtain concentration ranges of 0.40-50 µg/mL. Each concentration (100 µL) was added in a well (96-well micro plate) containing 100 µL of inoculum. An inoculum density of 1×10^6 cfu/mL of bacterial

TABLE-6
MICROBIAL GROWTH INHIBITORY POTENTIAL OF COMPOUNDS AND THE REFERENCE ANTIBIOTICS

Tested compounds	Concentration (µg/well)	Diameter of zone of inhibition (mm)/each well = 5 mm; Tested microorganisms					
		Gram-negative bacteria	Gram-positive bacteria			Fungus	Yeast
		Escherichia coli	*Bacillus cereus*	*Enterococcus faccium*	*Staphylococcus aureus*	*Aspergillus niger*	*Candida albicans*
PCPH	150	8	10	8	10	Not active	Not active
	100	7	8	6	8	Not active	Not active
Complex **1**	150	9	18	10	14	Not active	Not active
	100	7	16	7	11	Not active	Not active
HNSC	150	7	16	10	14	Not active	Not active
	100	6	14	8	12	Not active	Not active
Complex **2**	150	8	18	15	16	Not active	Not active
	100	7	15	13	15	Not active	Not active
Gentamycin	5	18	22	18	20	Not active	Not active
Nystatin	10	–	–	–	–	18	20
DMSO	30 µL	Not active	Not active	Not active	Not active	Not active	Not active

TABLE-7
MINIMUM INHIBITORY CONCENTRATION (µg/mL) OF THE COMPOUNDS AND REFERENCE ANTIBIOTIC (RA)

Tested compounds	Tested microorganisms					
	Gram-negative bacteria	Gram-positive bacteria			Fungus	Yeast
	Escherichia coli	*Bacillus cereus*	*Enterococcus faccium*	*Staphylococcus aureus*	*Aspergillus niger*	*Candida albicans*
PCPH	50	25	25	25	Inactive	Inactive
Complex **1**	12.5	6.12	12.5	12.5	Inactive	Inactive
HNSC	>50	25	50	50	Inactive	Inactive
Complex **2**	12.5	6.12	6.12	6.12	Inactive	Inactive
Gentamycin	5	5	5	5	Inactive	Inactive
Nystatin	–	–	–	–	10	10

strain was prepared in normal saline (9 g/L) by comparison with a 0.5 MacFarland turbidity standard with appropriate dilution [40]. The final concentration of DMSO in the well was less than 3%. The negative control well consists of 100 µL of MHB and 100 µL of the standard inoculum [41]. The plates were covered with sterile plate sealer, then agitated to mix the contents of the wells using a plate shaker and incubated at 37 ºC for 24 h. The assay was repeated three times. The MIC of sample was detected following additional (40 µL) of 0.2 mg/mL nitroblue tetrazolium chloride (NBT) (Himedia) to microplate wells and incubated at 37 ºC for 30 min [42]. Viable microorganisms reduced the yellow to black. MIC was defined as the lowest sample concentration of drug at which there was no visible growth of the organism.

Conclusion

The present work reports the synthesis, crystal structure, spectroscopic and DNA-binding and antimicrobial activity studies of pyridine-2-carboxaldehyde-*N*-(2-pyridyl)hydrazone (PCPH) Cu(II) complex $[Cu(PCPH)Cl(H_2O)](NO_3)(H_2O)_2$ (**1**) and 2-hydroxy-1-naphthaldehyde-semicarbazone (HNSC) Cu(II) complex $[Cu(II)(HNSC)H_2O]\cdot NO_3\cdot H_2O$ (**2**). Electronic absorption titration experiment, EB-DNA fluorescence quenching experiments, cyclic voltammetric experiments and viscosity measurements suggests that both Cu(II) complexes (**1** and **2**) might be non-intercalative surface or groove binder to ct-DNA. Agar diffusion method showed that both copper(II) complexes **1** and **2** have higher bacterial growth inhibitory potential than the corresponding ligand. The MIC for copper(II) complexes **1** and **2** in case of *Staphylococcus aureus*, *Bacillus cereus* and *Enterococcus faccium* were comparable with standard antibiotic.

ACKNOWLEDGEMENTS

The authors gratefully acknowledge UGC, New Delhi, India for financial support.

CONFLICT OF INTEREST

The authors declare that there is no conflict of interests regarding the publication of this article.

REFERENCES

1. S.D. Roughley and A.M. Jordan, *J. Med. Chem.*, **54**, 3451 (2011); https://doi.org/10.1021/jm200187y
2. M. Aldeghi, S. Malhotra, D.L. Selwood and A.W.E. Chan, *Chem. Biol. Drug Des.*, **83**, 450 (2014); https://doi.org/10.1111/cbdd.12260
3. T.J. Ritchie, S.J.F. Macdonald, R.J. Young and S.D. Pickett, *Drug Discov. Today*, **16**, 164 (2011); https://doi.org/10.1016/j.drudis.2010.11.014
4. T.J. Ritchie and S.J.F. Macdonald, *Drug Discov. Today*, **14**, 1011 (2009); https://doi.org/10.1016/j.drudis.2009.07.014
5. H.W. Boucher, G.H. Talbot, J.S. Bradley, J.E. Edwards, D. Gilbert, L.B. Rice, M. Scheld, B. Spellberg and J. Bartlett, *Clin. Infect. Dis.*, **48**, 1 (2009); https://doi.org/10.1086/595011

6. F. Gao, P. Yang, J. Xie and H. Wang, *J. lnorg. Biochem.*, **60**, 61 (1995); https://doi.org/10.1016/0162-0134(95)00002-6
7. S. Correia, P. Poeta, M. Hébraud, J.E. Capelo and G. Igrejas, *J. Med. Microbiol.*, **66**, 551 (2017); https://doi.org/10.1099/jmm.0.000475
8. V. Uivarosi, *Molecules*, **18**, 11153 (2013); https://doi.org/10.3390/molecules180911153
9. M. Imran, J. Iqbal, S. Iqbal and N. Ijaz, *Turk. J. Biol.*, **31**, 67 (2007).
10. W. Guerra, E. de Andrade Azevedo, A.R. de Souza Monteiro, M. Bucciarelli-Rodriguez, E. Chartone-Souza, A.M.A. Nascimento, A.P.S. Fontes, L. Le Moyec and E.C. Pereira-Maia, *J. Inorg. Biochem.*, **99**, 2348 (2005); https://doi.org/10.1016/j.jinorgbio.2005.09.001
11. R. Rohs, I. Bloch, H. Sklenar and Z. Shakked, *Nucleic Acids Res.*, **33**, 7048 (2005); https://doi.org/10.1093/nar/gki1008
12. A.-M. Stadler and J. Harrowfield, *Inorg. Chim. Acta*, **362**, 4298 (2009); https://doi.org/10.1016/j.ica.2009.05.062
13. M.J. Borah, R.K. Bhubon Singh, U.B. Sinha, T. Swu and P.J. Borah, *J. Chem. Crystallogr.*, **42**, 67 (2012); https://doi.org/10.1007/s10870-011-0205-5
14. W.B. Devi, R.K.B. Singh, J.P. Jasinski and J.A. Golen, *Inorg. Chem. Commun.*, **21**, 163 (2012); https://doi.org/10.1016/j.inoche.2012.05.006
15. U.I. Singh, R.K. Bhubon Singh, M.J. Borah, J.P. Jasinski and J.A. Golen, *J. Struct. Chem.*, **54**, 116 (2013); https://doi.org/10.1134/S0022476613010162
16. M. Nandy, D.L. Hughes, G.M. Rosair, R.K.B. Singh and S. Mitra, *J. Coord. Chem.*, **67**, 3335 (2014); https://doi.org/10.1080/00958972.2014.964697
17. R.K.B. Devi, S.P. Devi, R.K.B. Singh, R.K.H. Singh, T. Swu, W.R. Devi and C.H.B. Singh, *J. Coord. Chem.*, **67**, 891 (2014); https://doi.org/10.1080/00958972.2014.902449
18. N. Shantibala Devi, L. Jaideva Singh, S. Pramodini Devi, R.K. Bhubon Singh, R.K. Hemakumar Singh, B. Rajeswari and R.M. Kadam, *J. Mol. Struct.*, **1076**, 411 (2014); https://doi.org/10.1016/j.molstruc.2014.08.005
19. R.N. Patel, Y.P. Singh, Y. Singh, R.J. Butcher, M. Zeller, R.K.B. Singh and O. U-wang, *J. Mol. Struct.*, **1136**, 157 (2017); https://doi.org/10.1016/j.molstruc.2017.01.083
20. O. U-Wang, R.B. Singh, W.B. Devi, U.I. Singh, R.B. Devi, O.B. Devi, R. Shahani and T. Swu, *Inorg. Nano-Met. Chem.*, **49**, 363 (2019); https://doi.org/10.1080/24701556.2019.1661457
21. Agilent Technologies, CrysAlisPro, version 1.171.36.21; CrisAlis 171. Net, 10 Mead Road, Oxford Industrial Park, Yarnton, Oxfordshire, U.K. (2012).
22. G.M. Sheldrick, *Acta Crystallogr. A*, **64A**, 112 (2008); https://doi.org/10.1107/S0108767307043930
23. O.V. Dolomanov, L.J. Bourhis, R.J. Gildea, J.A.K. Howard and H. Puschmann, *J. Appl. Cryst.*, **42**, 339 (2009); https://doi.org/10.1107/S0021889808042726
24. D. Kivelson and R. Neiman, *J. Chem. Phys.*, **35**, 149 (1961); https://doi.org/10.1063/1.1731880
25. I.M. Procter, B.J. Hathaway and P. Nicholls, *J. Chem. Soc. A*, 1678 (1968); https://doi.org/10.1039/j19680001678
26. J.R. Wasson and C. Trapp, *J. Phys. Chem.*, **73**, 3763 (1969); https://doi.org/10.1021/j100845a034
27. A.W. Addison, T.N. Rao, J. Reedijk, J. van Rijn and G.C. Verschoor, *J. Chem. Soc., Dalton Trans.*, 1349 (1984); https://doi.org/10.1039/DT9840001349
28. M.E. Reichmann, S.A. Rice, C.A. Thomas and P.A. Doty, *J. Am. Chem. Soc.*, **76**, 3047 (1954); https://doi.org/10.1021/ja01640a067
29. J. Marmur, *J. Mol. Biol.*, **3**, 208 (1961); https://doi.org/10.1016/S0022-2836(61)80047-8
30. A. Wolfe, G.H. Shimer Jr. and T. Meehan, *Biochemistry*, **26**, 6392 (1987); https://doi.org/10.1021/bi00394a013
31. J.B. LePecq and C. Paoletti, *J. Mol. Biol.*, **27**, 87 (1967); https://doi.org/10.1016/0022-2836(67)90353-1
32. J. Liu, T. Zhang, T. Lu, L. Qu, H. Zhou, Q. Zhang and L. Ji, *J. Inorg. Biochem.*, **91**, 269 (2002); https://doi.org/10.1016/S0162-0134(02)00441-5
33. M. Lee, A.L. Rhodes, M.D. Wyatt, S. Forrow and J.A. Hartley, *Biochemistry*, **32**, 4237 (1993); https://doi.org/10.1021/bi00067a011
34. J.R. Lakowicz and G. Weber, *Biochemistry*, **12**, 4161 (1973); https://doi.org/10.1021/bi00745a020
35. Y. Li, Y. Wu, J. Zhao and P. Yang, *J. Inorg. Biochem.*, **101**, 283 (2007); https://doi.org/10.1016/j.jinorgbio.2006.10.004
36. W.D. Wilson, L. Ratmeyer, M. Zhao, L. Strekowski and D. Boykin, *Biochemistry*, **32**, 4098 (1993); https://doi.org/10.1021/bi00066a035
37. B.C. Baguley and M. Le Bret, *Biochemistry*, **23**, 937 (1984); https://doi.org/10.1021/bi00300a022
38. D.L. Boger, B.E. Fink, S.R. Brunette, W.C. Tse and M.P. Hedrick, *J. Am. Chem. Soc.*, **123**, 5878 (2001); https://doi.org/10.1021/ja010041a
39. C. Perez, M. Pauli and P. Bazerque, *Acta Biol. Med. Exp.*, **15**, 113 (1990).
40. V. Kuete, D.C. Fozing, W.F.G.D. Kapche, A.T. Mbaveng, J.R. Kuiate, B.T. Ngadjui and B.M. Abegaz, *J. Ethnopharmacol.*, **124**, 551 (2009); https://doi.org/10.1016/j.jep.2009.05.004
41. J.R. Zgoda and J.R. Porter, *Pharm. Biol.*, **39**, 221 (2001); https://doi.org/10.1076/phbi.39.3.221.5934
42. V. Kuete, B. Ngameni, C.C.F. Simo, R.K. Tankeu, B.T. Ngadjui, J.J.M. Meyer, N. Lall and J.R. Kuiate, *J. Ethnopharmacol.*, **120**, 17 (2008); https://doi.org/10.1016/j.jep.2008.07.026